

Efficient Selfconsistent Calculations of Multiband Superconductivity in UPd₂Al₃

P. M. Oppeneer¹ and G. Varelogiannis²

¹*Institute of Solid State and Materials Research, P.O. Box 270016, D-01171 Dresden, Germany*

²*Department of Physics, National Technical University of Athens, GR-15780 Athens, Greece*

(Dated: February 1, 2008)

An efficient physically motivated computational approach to multiband superconductivity is introduced and applied to the study of the gap symmetry in a heavy-fermion, UPd₂Al₃. Using realistic pairing potentials and accurate energy bands that are computed within density functional theory, self-consistent calculations demonstrate that the only accessible superconducting gap with nodes exhibits *d*-wave symmetry in the *A*_{1g} representation of the *D*_{6h} point group. Our results suggest that in a superconductor with gap nodes the prevailing gap symmetry is dictated by the constraint that nodes must be as far as possible from high-density areas.

PACS numbers: PACS numbers: 74.25.Jb, 74.20.-z

Superconductivity (SC) in heavy-fermion (HF) materials exhibits a fascinating complexity of phenomena [1]. The nature of the SC state is mostly anticipated to be unconventional, i.e., an additional symmetry is broken in the SC state, and the order parameter is therefore not the conventional spin singlet *s*-wave type [2, 3]. The identification of the order parameter symmetry is an essential issue in current studies of unconventional SC. A common approach to address the symmetry of the order parameter is through investigations of the SC gap, which is expected to have the same symmetry as the order parameter. While progress has been made for high-*T*_c superconductors (HTSC), the identification of the gap symmetry remains an open question for most HF materials. The eventual identification of the gap symmetry in a HF compound is, however, not sufficient to identify the pairing mechanism. Additional elements are necessary and in the case of HF materials, it was suggested that spin fluctuations - either in the itinerant [4, 5] or localized limit as magnetic excitons [6, 7] - may replace the phonons as mediators of the pairing.

In order to identify the gap symmetry and clarify its relationship to the pairing mechanism, selfconsistent solutions of the SC gap equations with physical momentum dependent pairing potentials and accurate band structures are unavoidable (*cf.* [8, 9]). Unfortunately, in the case of HF's the situation is rather complex. In addition to the three-dimensionality, we must deal with several anisotropic bands that cross the Fermi level (*E*_F) producing numerous highly anisotropic Fermi surface (FS) sheets. As a consequence, no realistic selfconsistent calculations of SC have been achieved so far in HF materials.

Here we introduce a computational approach to multiband SC in a HF material, by directly combining relativistic band-structure calculations with a physically motivated procedure to solve efficiently and accurately the multiband BCS gap equation selfconsistently. The efficiency of our procedure allows a systematic study of the influence of the momentum structure of the pairing on the resulting gap symmetry in an anisotropic multiband

system. We focus on UPd₂Al₃ which is a fascinating HF superconductor having a moderately large specific heat coefficient $\gamma = 140$ mJ/mol K², and a relatively high critical temperature *T*_c = 2 K [10]. It orders antiferromagnetically below *T*_N = 14.3 K with an ordered moment of 0.85 μ_B /U-atom [11], which is large compared to the moments of other HF superconductors as, e.g., UPt₃, which has a moment of only 0.03 μ_B [12]. A further anomalous feature is that the antiferromagnetic (AFM) order coexists with SC below 2 K. Coexistence of magnetism and SC was observed for other materials, e.g., containing 4*f* elements, but in those cases the magnetism is due to the localized 4*f* electrons far from *E*_F, whereas the SC is carried by itinerant electrons at *E*_F. Conversely, for UPd₂Al₃ most of the recent studies reveal that the SC, magnetic order, as well as HF behavior *all* involve the uranium 5*f* states [13, 14].

Previous investigations revealed that UPd₂Al₃ can be classified as a spin singlet, BSC-type superconductor [15, 16, 17]. The appropriate starting point is therefore the coupled multiband BCS gap equation [18], for *T* → 0:

$$\Delta_n(\mathbf{k}) = - \sum_{n'} \sum_{\mathbf{k}'} \frac{V_{nn'}(\mathbf{k}, \mathbf{k}') \Delta_{n'}(\mathbf{k}')}{2 [E_{n'\mathbf{k}'}^2 + |\Delta_{n'}(\mathbf{k}')|^2]^{1/2}}, \quad (1)$$

where Δ_n is the gap of band *n*, and *E*_{*n*} is the corresponding singleparticle energy relative to *E*_F. *V*_{*nn'*} is the pairing potential. The coupled multiband gap equation is at present too complicated to be solved numerically on the real FS of the material and with physical momentum-dependent pairing potentials. However it is a common experimental practice not to consider a gap symmetry defined separately for each band, but to work with a “global” gap symmetry valid for all bands, i.e., defined in the whole Brillouin zone (BZ) (see, e.g., [12, 19, 20]). Our goal is to compute selfconsistently such global gap symmetry. To achieve this goal, one could proceed as follows: solve for each individual band the singleband BCS gap equation, and subsequently, combine and interpolate these singleband gaps to a generalized gap $\Delta(\mathbf{k})$ defined in the whole BZ. This is precisely what we do by solving

as an *ansatz* a modified gap equation

$$\Delta(\mathbf{k}) = - \sum_{\mathbf{k}'} \frac{V(\mathbf{k}, \mathbf{k}') \Delta(\mathbf{k}')}{2 [G(\mathbf{k}') + |\Delta(\mathbf{k}')|^2]^{1/2}}, \quad (2)$$

with $G(\mathbf{k}) \equiv (1/E_{n_1\mathbf{k}}^2 + 1/E_{n_2\mathbf{k}}^2 + \dots)^{-1}$. On the FS sheet of band n , $G_{\mathbf{k}}$ is equal to $E_{n\mathbf{k}}^2$, and thus $\Delta(\mathbf{k}) = \Delta_n(\mathbf{k})$. Note that intraband as well as interband processes are taken into consideration. A simplification specific to UPd₂Al₃ has been implemented in Eq. (2) which could, however, be relaxed. Since all bands at E_F have mainly $5f$ character [13], there is no need to discriminate different band dependencies in the pairing potential, which we thus assume to be identical for all n .

The energy dispersions $E_n(\mathbf{k})$ were computed within the framework of density functional theory in the local spin-density approximation (LSDA). Knöpfle *et al.* [13] demonstrated a very close agreement between the measured [21] and calculated in this framework de Haas-van Alphen frequencies. Consequently, the FS of UPd₂Al₃ is accurately described by the LSDA energy dispersions. Since the relevant physics for SC happens in the vicinity of the FS, the LSDA energies provide the appropriate input for our investigation of the gap symmetry. We computed the LSDA energy bands of UPd₂Al₃ using the relativistic augmented-spherical-wave method [22]. The resulting band structure of UPd₂Al₃ along characteristic symmetry lines is shown in Fig. 1 for the paramagnetic and AFM state. The FS resulting from our AFM bands consists of four types of sheets, and is practically identical to that computed previously [13], as is also the ordered AFM moment of $0.81 \mu_B$, which agrees with the experimental moment of $0.85 \mu_B$ [11].

For the pairing potential we consider here two categories of pairing kernels that are generally accepted and were shown to produce unconventional order parameters. The small- q pairing potential, adopts at small wavevectors $\mathbf{k} - \mathbf{k}'$ the following form in momentum space $V(\mathbf{k}, \mathbf{k}') = \frac{-V}{q_c^2 + (\mathbf{k} - \mathbf{k}')^2} + \mu^*(\mathbf{k} - \mathbf{k}')$. This kernel is characterized by a smooth momentum cut-off q_c which selects the small- q processes in the attractive part [23, 24, 25, 26, 27]. At larger wavevectors the repulsive Coulomb pseudopotential $\mu^*(\mathbf{k} - \mathbf{k}')$ may prevail. This type of attractive interaction may be due to *phonons* if the system is close to instabilities and screening with short range Hubbard-like Coulomb terms is involved [25]. It has been claimed that this type of kernel may account for unconventional SC in HTSC [23, 24, 25, 26, 27] and in other materials, including HF's [25]. Agterberg *et al.* [28] have recently suggested for HF superconductors a multipocket FS with an attractive intrapocket and repulsive inter-pocket potential. Such situation results naturally from a potential dominated by small- q attractive pairing as the one considered here, if the FS contains multipockets separated in momentum space. We also considered the case of pairing mediated by *spin fluctuations* using a

phenomenological Millis-Monien-Pines pairing potential [29] which has the form $V(\mathbf{k}, \mathbf{k}') = \frac{V}{q_c^2 + (\mathbf{k} - \mathbf{k}' - \mathbf{Q})^2}$ where $\mathbf{Q} = \pm(0, 0, \pi/2c)$ in UPd₂Al₃ (c is the c axis lattice constant). The \mathbf{Q} value was verified by neutron scattering experiments [30]. Pairing through spin fluctuations has been suggested for virtually all unconventional SC's, including UPd₂Al₃ [14, 17].

To obtain a selfconsistent solution of our modified gap equation with such momentum dependent kernels and the original LSDA bands we have used a Fast-Fourier-Transform technique. The problem is solved iteratively on a symmetric part of the BZ that we discretize with a $128 \times 128 \times 128$ momentum grid. For each point of our 3-D grid we have our LSDA energy bands as an input. Within our procedure the momentum space problem is fully resolved numerically without any simplification or bias on the resulting gap symmetry.

The accessible even parity gap states can possess s - or d -wave symmetry. As UPd₂Al₃ and thus our LSDA bands obey the hexagonal D_{6h} point group symmetry, the accessible gap states of d -wave symmetry that have nodes should transform according to the irreducible representations of the D_{6h} group [31] shown schematically in Fig. 2. In our calculations we used the small- q phonon pairing potential with various parameter choices for both the paramagnetic and AFM energy bands and the spin-fluctuations pairing potential only for the AFM bands. An initial gap configuration is chosen randomly and the system converges within the iteration cycle towards the most favorable solution. Also, we adopted as initial gap each of the representations in Fig. 2 and tried if the system would converge towards the chosen configuration. Depending on the parameters in pairing kernel (q_c , V , μ^*), we can achieve as selfconsistent solution either a gap having s -wave or d -wave symmetry. Quite unexpectedly, in the latter case we find that *the only accessible gap state with nodes in UPd₂Al₃ belongs to the irreducible representation A_{1g}* . No other representation possessing nodes was accessible for all the parameters in both types of pairing kernels.

We show in Fig. 3 some examples of our selfconsistently computed gap functions in the plane H – A – H, H – K – H which contains the z axis (the A – Γ – A axis) and in the plane obtained by a $\pi/6$ or $\pi/2$ rotation around the z axis (the plane L – A – L, L – M – L). All selfconsistent solutions shown in Fig. 3 have two lines of nodes perpendicular to the A – Γ – A axis, thus belonging in the A_{1g} representation. To study the influence of the coexisting AFM order on SC we have made calculations using both paramagnetic and AFM bands. In both paramagnetic and AFM cases, the only solutions with gap nodes are of A_{1g} type. We note that our results with the spin-fluctuations kernel confirm the model analyses performed by Huth *et al.* [17] and Bernhoeft [14]. In particular, Bernhoeft predicted for SC mediated by spin fluctuations in UPd₂Al₃ a characteristic symmetry prop-

erty of the global gap, *viz.* $\Delta(\mathbf{k}) = -\Delta(\mathbf{k} + \mathbf{Q})$, which, in its simplest form, would be fulfilled by a gap having the functional dependence $\Delta(\mathbf{k}) \propto \cos(k_z c)$. Our gap computed selfconsistently with the spin-fluctuation pairing kernel does obey this symmetry property, and the shape of the gap does correspond closely to $\cos(k_z c)$ (see Fig. 3). In addition, we find here that small- q phonon pairing may lead to the same d -wave A_{1g} state, demonstrating that there is not a one-to-one correspondence between the gap symmetry and a specific microscopic mechanism, although experiments suggest that spin degrees of freedom are likely involved in the pairing [6, 30, 32].

There is overwhelming experimental evidence that indeed UPd₂Al₃ has a gap with the A_{1g} node structure. Recent tunnel measurements along the z axis showed the absence of a node in this direction [20]. However, the presence of nodes is definitely established for UPd₂Al₃, and since A_{1g} is the only even parity gap with nodes which is nodeless along the z direction (see Fig. 2), it was deduced *a posteriori* that the gap symmetry must be A_{1g} type [20]. In addition, the observation [30, 32] of a spin-fluctuations peak below T_c at $(0, 0, \pi/2c)$ would be forbidden by the involved coherence factors unless the gap changes sign along the z axis as in the A_{1g} representation. Finally, measurements of the angular dependence of the critical field indicate two lines of nodes perpendicular to the z axis [19] again suggesting the A_{1g} representation. UPd₂Al₃ is one of the few HF superconductor for which such a clear picture of the nodal structure of the gap is obtained from the experiments. We consider the agreement of our results with the experiments as strong support of our calculations.

The surprising robustness of the A_{1g} solution results from the following general rule: If a system must choose a gap symmetry with nodes because of the repulsive effective interaction at large wavevectors (short distances) it chooses *the representation that has the minimum number of nodes as far as possible from the high-density areas*. In fact, the system must *maximize* the condensation free energy and this is obtained when there is a gap in the high-density areas and the node (gapless) areas are kept minimal. Examining the paramagnetic bands of UPd₂Al₃ (Fig. 1b) we see that the high-density areas near the FS due to saddle points in the band dispersions are found essentially near the A point and near the H point. The A_{1g} representation prevails because it is the only one *without a node near the A point*. In the case of the AFM bands (Fig. 1c), the saddle points of the bands near the FS are found essentially in the $z = 0$ plane (near the Γ point, along the $\Gamma - K$, $K - M$ and $M - \Gamma$ symmetry lines) and near the Γ point along $\Gamma - A'$ ($A' = A/2$). The high-density areas in the $z = 0$ plane exclude the B_{1g} , E_{1g} and B_{2g} representations which have a line node in the $z = 0$ plane. From the remaining A_{1g} , E_{2g} and A_{2g} representations, A_{1g} is the only one without a line of nodes parallel to the $A - \Gamma - A$ axis which would cross the

high-density areas at Γ and near Γ along $\Gamma - A'$. Also, due to the AFM symmetry a high density occurs again at A, as A is equivalent to Γ . The node perpendicular to the $\Gamma - A$ path in the A_{1g} representation is close to A' and therefore does not cross the high-density areas near Γ and A. Note that A_{2g} , B_{1g} and B_{2g} are also handicapped by the fact that they have more nodal areas.

To stress the generality of this argument we reconsidered the case of cuprate HTSC. Saddle points produce high-density areas in the vicinity of $(0, \pi/a)$ and symmetry related areas (a is the basal-plane lattice constant). The $d_{x^2-y^2}$ gap symmetry corresponds to nodes along the $(\pi/a, \pi/a)$ direction as far as possible from the high-density $(0, \pm\pi/a)$ and $(\pm\pi/a, 0)$ areas. Using both types of pairing kernels as adopted for UPd₂Al₃ (now $\mathbf{Q} = (\pi/a, \pi/a)$) we were never able to obtain a d_{xy} solution for which the nodes cross the high-density $(0, \pi/a)$ areas *no matter the details of the interaction*.

In conclusion, we have proposed an efficient computational approach to the multiband gap equation. Our selfconsistent calculations of the gap in UPd₂Al₃ demonstrate that the only accessible gap symmetry with nodes transforms according to the A_{1g} irreducible representation of the D_{6h} point group, independent of whether the pairing potential is dominated by small- q attractive processes involving phonons or by spin fluctuations. The robustness of the A_{1g} representation is analyzed to be due to the presence of high-density regions of the relevant bands in the vicinity of the Γ and A points, that preclude node formation at these points. As a general rule we obtain that nodes must be as far as possible from high-density areas in the phase space.

We are grateful to H. Adrian, N. Bernhoeft, P. Fulde, M. Huth, M. Lang, P. Thalmeier, N. Sato and F. Steglich for illuminating discussions. We thank M. Huth for the figure of the irreducible representations of the D_{6h} group.

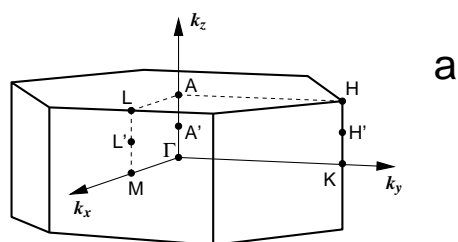
-
- [1] F. Steglich *et al.*, Phys. Rev. Lett. **43**, 1892 (1979).
 - [2] M. Sigrist and K. Ueda, Rev. Mod. Phys. **63**, 239 (1991).
 - [3] J.F. Annett, Adv. Phys. **39**, 83 (1991).
 - [4] N.D. Mathur *et al.*, Nature **394**, 39 (1998).
 - [5] S.S. Saxena *et al.*, Nature **406**, 587 (2000).
 - [6] N. Sato *et al.*, Nature **410**, 340 (2001).
 - [7] P. Thalmeier, Eur. Phys. J. B **27**, 29 (2002).
 - [8] W.M. Temmerman *et al.*, Phys. Rev. Lett. **76**, 307 (1996); B.L. Gyorffy *et al.*, Phys. Rev. B **58**, 1025 (1998).
 - [9] I.I. Mazin and D.J. Singh, Phys. Rev. Lett. **82**, 4324 (1999).
 - [10] C. Geibel *et al.*, Z. Phys. B **84**, 161 (1991).
 - [11] A. Krimmel *et al.*, Z. Phys. B **86**, 161 (1992).
 - [12] R. Joynt and L. Taillefer, Rev. Mod. Phys. **74**, 235 (2002).
 - [13] K. Knöpfle *et al.*, J. Phys.: Condens. Matter **8**, 901 (1996).
 - [14] N. Bernhoeft, Eur. Phys. J. B **13**, 685 (2000).

- [15] A. Amato *et al.*, Europhys. Lett. **19**, 127 (1992).
- [16] M. Kyougaku *et al.*, J. Phys. Soc. Jpn. **62**, 4016 (1993).
- [17] M. Huth, M. Jourdan, and H. Adrian, Eur. Phys. J. B **13**, 695 (2000).
- [18] H. Suhl, B.T. Matthias, and L.R. Walker, Phys. Rev. Lett. **3**, 552 (1959).
- [19] J. Hessert *et al.*, Physica B **230–232**, 373 (1997).
- [20] M. Jourdan, M. Huth, and H. Adrian, Nature **398**, 47 (1999).
- [21] Y. Inada *et al.*, Physica B **189–200**, 119 (1994).
- [22] A.R. Williams, J. Kübler, and C.D. Gelatt, Phys. Rev. B **19**, 6094 (1979).
- [23] G. Varelogiannis *et al.*, Phys. Rev. B **54**, R6877 (1996).
- [24] A.A. Abrikosov, Phys. Rev. B **53**, R8910 (1996); *ibid* **54**, 446 (1997); Physica C **222**, 191 (1994).
- [25] G. Varelogiannis, Phys. Rev. B **57**, 13743 (1998).
- [26] M. Weger and M. Peter, Physica C **317–318**, 252 (1999).
- [27] A.J. Leggett, Phys. Rev. Lett. **83**, 392 (1999).
- [28] D.F. Agterberg, V. Barzykin, and L.P. Gor'kov, Phys. Rev. B **60**, 14868 (1999).
- [29] A.J. Millis, H. Monien, and D. Pines, Phys. Rev. B **42**, 167 (1990).
- [30] N. Bernhoeft *et al.*, Phys. Rev. Lett. **81**, 4244 (1998).
- [31] S.K. Yip and A. Garg, Phys. Rev. B **48**, 3304 (1993).
- [32] N. Metoki *et al.*, Phys. Rev. Lett. **80**, 5417 (1998).

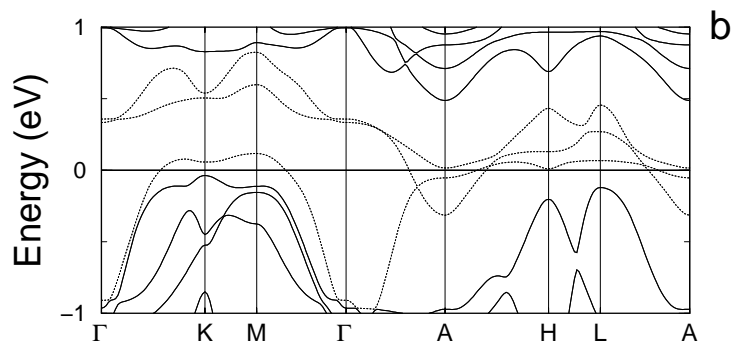
FIG. 1: (a) The hexagonal Brillouin zone with high symmetry points. In the AFM phase the BZ is reduced by a factor two along the z axis (denoted by the primed letters). (b) The energy bands along high symmetry directions in the paramagnetic, and (c) the AFM phase of UPd_2Al_3 . The relevant bands for superconductivity are shown by the dotted lines.

FIG. 2: The even parity d -wave-type irreducible representations of the D_{6h} point group. While in principle all are accessible for the gap, only the A_{1g} results from our selfconsistent gap calculations.

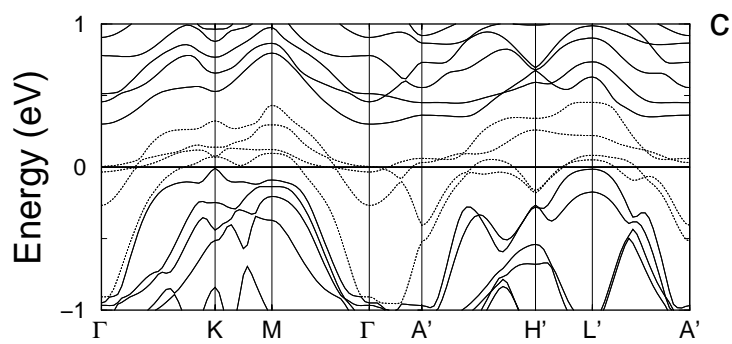
FIG. 3: Examples of the selfconsistent solutions of the gap equation in characteristic planes (with sides indicated) containing the Γ point (in the center) and the z axis. The thick black lines show the nodes and in the dark gray areas the gap is negative. All nodes cut the z axis as in the A_{1g} representation. Shown are gaps computed with the small- q pairing and paramagnetic energy bands (a), and the spin-fluctuations pairing and AFM bands, (b) and (c).



a

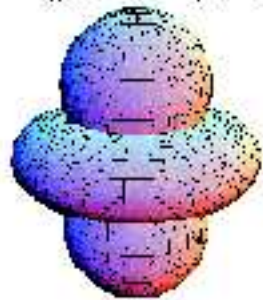


b

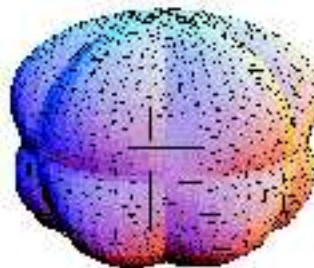


c

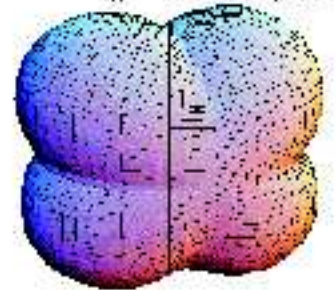
$$A_{1g}: (k_x^2 + k_y^2) - k_z^2$$



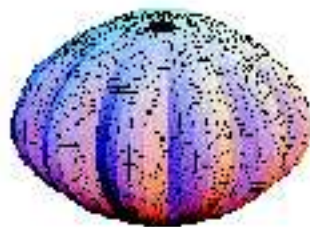
$$B_{1g}: k_z k_x (k_x^2 - 3k_y^2)$$



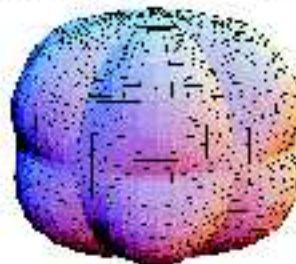
$$E_{1g}: k_x k_z + k_y k_z$$



$$A_{2g}: k_x k_y (k_x^2 - 3k_y^2) (k_y^2 - 3k_x^2)$$



$$B_{2g}: k_z k_y (k_y^2 - 3k_x^2)$$



$$E_{2g}: k_x^2 - k_y^2 + 2 k_x k_y$$

